# High Solids Content Emulsions. I. A Study of the Influence of the Particle Size Distribution and Polymer Concentration on Viscosity

**M. SCHNEIDER, J. CLAVERIE, C. GRAILLAT, T. F. MCKENNA**

LCPP-CNRS/ESCPE-Lyon, Bât. 308F, 43 Blvd du 11 Novembre 1918, 69616 Villeurbanne Cedex, France

*Received 14 June 2001; accepted 10 September 2001*

**ABSTRACT:** An experimental and modeling study was carried out to understand the relationship between the viscosity of a multimodal latex and its particle-size distribution (PSD) and polymer concentration. This study illustrates the inadequacy of existing models in predicting the viscosity of complex latices. It is shown that the latex viscosity at a fixed shear rate is very sensitive to the polymer concentration at high solids content and to the PSD. © 2002 Wiley Periodicals, Inc. J Appl Polym Sci 84: 1878–1896, 2002; DOI 10.1002/app.10511

**Key words:** particle-size distribution; latex; viscosity; multimodal PSD

## INTRODUCTION

Recent studies of high solids content latices (e.g., refs. [1] and [2]) have shown that it is possible to obtain polymer volume fractions of well over 65%, and occasionally over 70%, by correctly manipulating the particle-size distribution (PSD) of the final product. One can achieve these levels of solids content essentially by creating bimodal or trimodal latices, where 60–80% of the polymer phase is composed of large particles (>500–600 nm), and the remaining particles are between four and eight times smaller. Chu et al.[3] showed that the viscosity of this type of concentrated, multimodal dispersion can be very sensitive to the PSD and solid content. In what follows, we will present an experimental study of the rheological characteristics of high solids content latices, along with a preliminary attempt at quantifying the impact of PSD and solids content on the latex viscosity.

*Correspondence to:* T. F. McKenna (mckenna@cpe.fr).
Contract grant sponsor: Atofina (CERDATO).

Journal of Applied Polymer Science, Vol. 84, 1878–1896 (2002)
© 2002 Wiley Periodicals, Inc.

As a large number of latex products are used in the form of films, high viscosities are undesirable from an applications point of view because they lead to long film drying times and make the application of the latex on a surface problematic. In addition, high viscosity can lead to a drastic reduction in the quality of the mixing in the semibatch stirred tank reactors typically used in latex preparation, and transfer of the latex from the reactor to other parts of the plant can be difficult when the viscosity of the fluid increases above a certain limit (see, e.g., ref. [4]) For these reasons, it is important to control the PSD of a multimodal latex and to understand the relationship between the PSD, the solids content, and the viscosity.

Emulsion polymer latices will exhibit viscoelastic rheological characteristics when the forces between the particles are relatively strong, as is the case with high solids content latices (i.e., with polymer volume fractions > 55–60%). Trying to quantify the rheological behavior of a colloidal dispersion essentially boils down to trying to determine the influence of the size, nature, and concentration of the particles.[5–8] Adding particles to a homogeneous fluid forces us to consider as-

**Table I Relative Viscosity of a Dispersion as a Function of the Particle Volume Fraction**

| | |
|---|---|
| Vand (1945)[9] | $\eta_r = 1 + 2.5\phi + k_2\phi^2$ ($k_2$ between 2.5 and 9) |
| Mooney (1951)[10] | $\eta_r = \exp\left(\frac{2.5\phi}{1 - \phi/\phi_{max}}\right)$ |
| Krieger & Dougherty (1972)[11] | $\eta_r = (1 - \phi/\phi_{max})^{-[\eta]\phi_{max}}$ |
| Quemada (1978)[12] | $\eta_r = \left(1 - \frac{[\eta]}{2}\phi\right)^{-2}$ |

pects linked to (i) the Brownian movement of the particles; (ii) the hydrodynamic flow field around the particles; and (iii) the interactions between the particles in the fluid.

## Theoretical Treatments

One of the first attempts to describe the influence of the presence of particles in a dispersion was the well-known Einstein equation:

$$\eta_r = 1 + 2.5\phi \quad (1)$$

This expression linked the relative viscosity of the dispersion ($\eta_r$, viscosity of the dispersion relative to the viscosity of the solvent) to the volume fraction of spherical particles in suspension ($\phi$). This expression is only valid for highly dilute suspensions ($\phi < 0.01$) and is valid only if the following conditions are satisfied:

1. The particles remain far enough apart that they do not interact and that the flow field created around a given particle does not impinge upon that of the neighboring particles.
2. The suspended particles are considered to be rigid, uniform spheres.
3. The no-slip boundary condition applies at the surface of the particles.
4. The dispersion is in a Stokes flow regime.
5. The solvent is an incompressible Newtonian liquid, and the molecules of the solvent are very small with respect to the radius of the particles.
6. The influence of exterior forces (e.g., gravity) is negligible.

Although the last two hypotheses might be acceptable from the point of view of modeling latex viscosity, the first four are not, and the fact that we are not interested in extremely dilute dispersions means that eq. 1 is not useful for high solids content systems. In the case of concentrated dispersions, the close proximity of the particles means that there will be a physical interaction between neighboring particles and that the flow field around a given particle can modify (or interact with) that around its neighbors. A number of authors (e.g., refs. [9–12]) have tried to adapt the approach used in developing eq. 1 by proposing empirical equations of the form $\eta_r = f(\phi)$ to account for the effects of increased concentration. Four of these are summarized in Table I.

Perhaps the best known of the equations used to describe the effect of particle concentration on the relative viscosity in Table I is the Mooney equation. It is based on purely geometric considerations. It accounts for the increase in viscosity due to the addition of new particles by considering the viscosity of the original dispersion as that of the solvent. Note though that this approach is still based on the assumption that the particles in the dispersion are of a uniform size. Although this equation functions correctly for a number of applications, it is not particularly well-adapted to the problem at hand for a number of reasons, including the fact that in a typical polymer latex, particle–particle interactions are influenced by the electrostatic nature of the particle stabilizers (electroviscous effects), as well as the fact that we are interested in latices composed of particles of different sizes.

Three different electroviscous phenomena can be caused by the electrostatic stabilization systems commonly used in emulsion polymerization, and the consequent electric double layer that surrounds the particles, and can contribute to an increase in the viscosity of a emulsion. The first of these phenomena is the distortion of the double layer when the particle is subjected to a hydrodynamic constraint. This can provoke an asymmetry in the electric field around the particles, but is in general, a relatively weak contribution. The

second contribution is linked to interparticulate colloidal interactions and can be thought of by considering an effective particle radius. The weaker the ionic force in the latex, the thicker the electric double layer around the particles will be. The volume effectively occupied by a given particle will therefore be a function of the ionic strength of the latex. This effect can be quite significant at high concentrations, where the viscosity is a very strong function of the volume fraction of polymer. The third electroviscous effect is important when the milieu contains polyelectrolytes absorbed onto the surface of the particles. These chains can unfold and become charged under different conditions (pH, electric properties of the continuous phase, etc.). This unfolding of the chains on the surface of the particles can modify the interaction between the particles and between the particles and the continuous phase.

The models listed in Table I, as well as the Einstein equation, do not account for particle–particle, or particle–fluid interactions, and therefore implicitly assume that electroviscous effects are not important. This simplification is equivalent to saying that the viscosity of a dispersion is independent of the size of the dispersed particles, which, as we will see below, is not the case as we are concerned with colloidal particles with electric surface charges.

In so far as the influence of particle size is concerned, experience has shown that, in practice, a latex of small particles is more viscous than a latex of larger particles, all other things being equal. The reason for this is that for a given concentration, the smaller the particles are, the more numerous they are and the more the effect of interparticle interactions is important because the distance between particles is reduced. Also, the thickness of the electric double layer, $\kappa^{-1}$, can be calculated as follows[13]:

$$1/\kappa = \sqrt{\frac{\varepsilon k_B T}{8\pi e^2 N_A I}} \qquad (2)$$

where $\epsilon$ is the dielectric constant of water (continuous medium), $k_B$ is the Boltzman constant, $T$ is the absolute temperature, $I$ is the ionic strength, $e$ is the charge of a single electron, and $N_A$ is Avagadro's number. The thickness of the layer is independent of the particle size and will therefore have a relatively larger impact when the particles are small.

If we reconsider the equations presented in Table I, we can see that the expressions proposed by Mooney and by Krieger and Dougherty contain a term $\phi_{max}$, which represents the maximum volume fraction of spheres in the dispersions. Once the effective volume fraction is equal to $\phi_{max}$, the viscosity of the latex will tend toward infinity. In a slightly different vein, Bicerano et al.[14] claim that $\phi_{max}$ can be used as an approximation for what they call the viscosity percolation threshold ($\phi^*$) because they prefer to use the percolation theory to understand the influence of particle size, shape, and concentration on the viscosity of a dispersion of particles. $\phi^*$ is said to be the volume fraction of particles at which the particles in the dispersion are stuck in place. They argue that viscosity should be modeled with respect to the reduced volume fraction of particles (i.e., the term $\phi/\phi_{max}$ that appears in some of the equations in Table I) rather than just $\phi$. Ideally, it would be interesting to be able to attach a real physical significance to this term to help understand the limits of solid content beyond which we cannot hope to go if we wish to avoid problems with high viscosity. From the point of view of the viscosity of a dispersion of particles, and in particular of a multimodal latex, it is intuitively obvious that the combination of particle sizes that provides the highest value of $\phi_{max}$ will also lead to the lowest viscosity for a fixed value of $\phi$. For this reason, it is interesting for us to identify a value of $\phi_{max}$ for our multimodal latices and to find a means of quantifying the relationship between the PSD, polymer concentration, and $\phi_{max}$.

For the case of uniform spheres in an infinitely large container, the value of $\phi_{max}$ would be 0.74, which corresponds to the case of compact, cubic-centered packing of particles. However, if $\phi_{eff} = 0.74$, then the latex would have an infinite viscosity. On the other hand, a sphere with the same diameter as one edge of a cubic container would occupy a volume fraction of $\phi = 0.52$. Clearly, it is unlikely that the particles in a polymeric dispersion would arrange themselves in either of these fashions, and we can expect the value of $\phi_{max}$ to be somewhere between these limits for a monomodal latex (note that this is not true for a multimodal latex because small particles can insert themselves in the spaces between the larger ones, thereby increasing $\phi_{max}$ above the limit of 0.74).

By convention, it is accepted that a random packing of uniform spheres will lead to a volume fraction of 0.64. However, Greenwood et al.[15] pointed out that this value is in fact an average

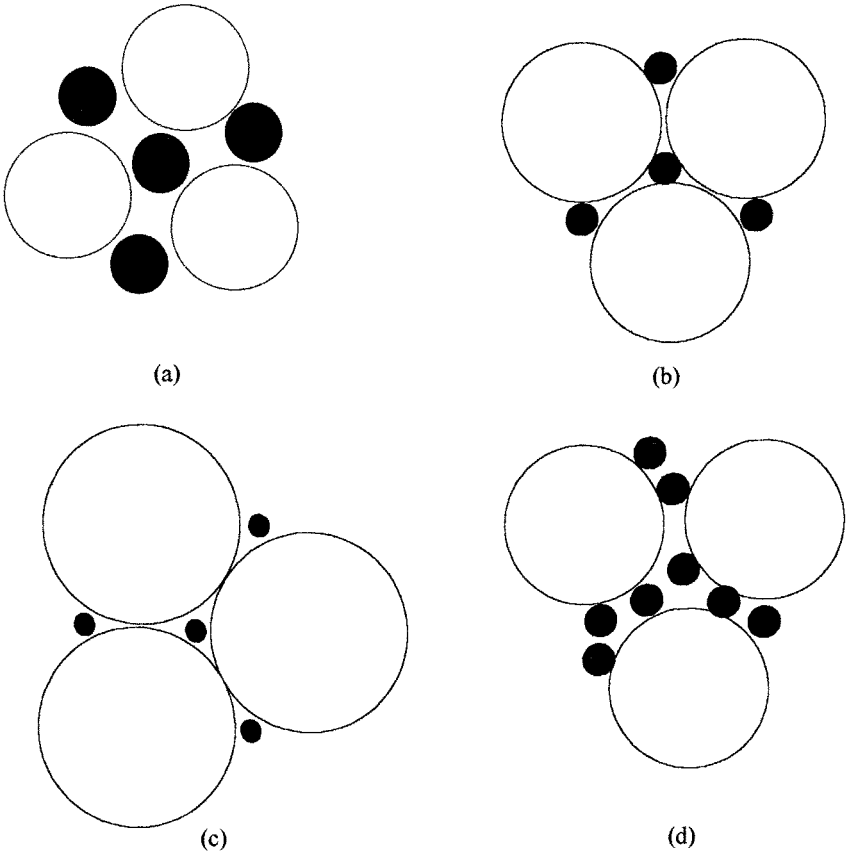


**Figure 1** Schema of relationship between particle size, concentration, and solids content ($\phi_{max}$) in two dimensions. Choosing the correct ratio of diameters allows us to minimize the space lost between the particles in Figure 1(b). In (a), the small particles are too large to fit in the interstices between the large particles, and in (c), they are too small. In addition, even if the diameter ratio is correct, there are too many small particles in (d) to obtain the maximum value of $\phi_{max}$. Note that the reasoning is the same in three dimensions, only the diameter ratio will change.

value. Some random packings will lead to higher values of $\phi$, others to lower values. For example, values of up to 0.68 were observed in certain cases of random packing.[16] In fact, Torquato proposed (see ref. [16]) that rather than treating the problem as trying to identify the maximum volume fraction of a randomly packed set of spheres, it is more useful to consider the problem in terms of frozen packings (i.e., configurations or arrangements of spheres that cannot be moved by an external force). Torquato believes that this type of packing exists and can even correspond to relatively low volume fractions of spheres. We will return to this point below.

Further difficulties arise from the fact that latices in general, and the bimodal high solids content latices that interest us here, are not characterized by a monodisperse PSD, but rather contain a number of particles of different sizes. As we mentioned above, the underlying idea behind creating bi- or trimodal latices is to insert small particles into the spaces between the bigger ones, in other words, to increase the value of $\phi_{max}$. The upper limit of $\phi_{max}$ will depend to a large extent on the average particle sizes in the medium, as well as on the relative concentration of each population in the latex. This is illustrated schematically in Figure 1 in two dimensions (the reasoning will be the same in three dimensions). If we compare the situations in Figure 1(a–c), it is clear that there will be an optimum ratio of the diameter of large particles to small particles that allows us to obtain the highest possible value of $\phi_{max}$. In Figure 1(a), the small particles are too large to fit between the larger ones, and in Figure 1(c), they are too small and do not entirely fill up

the interstices between the large particles. In addition, we can also compare Figure 1(b) and 1(d). In Figure 1(b), the small particles are just large enough, and there are just enough of them to fill up the interstices, but still allow the larger particles to occupy a maximum space. In Figure 1(d), we have the same particle size ratio as in Figure 1(b), but there are more small particles. This has the same effect as in Figure 1(a), where the small particles once again stop the larger ones from occupying the most space possible.

It should be clear from this discussion that the direct calculation of the value of $\phi_{max}$ for a multimodal latex can be quite difficult. Given that it took almost four centuries to prove Kepler's original hypothesis that $\phi_{max} = 0.74$ for uniform spheres (posed in 1609),[17] it is reasonable to say that it is beyond the scope of the current article to attempt an *a priori* mathematical calculation of $\phi_{max}$ for bimodal and trimodal latices. For this reason, it is preferable to test different packings, either experimentally or by simulation, to quantify the relationship between the PSD, concentration of different particle populations, and $\phi_{max}$ (e.g., as done by Sudduth[18,19]). This implies that we will only be able to consider randomly packed configurations, and, given the discussion in ref. [16], means that it will be impossible to find an absolute value for $\phi_{max}$ for a given latex. We will come back to this notion of identifying the maximum volume fraction, and its implications in terms of the latex viscosity below.

Other attempts were made to model the influence of the PSD of a multimodal latex on its viscosity. For example, Farris[20] developed an approach to predict the reduced viscosity of a multimodal mixture. This model was developed and tested for mixtures of monomodal distributions of spheres, and, in theory, can be adapted to any number of subpopulations of the PSD provided that each one is monodisperse. We will briefly present this model here for the case of a trimodal latex containing small (S), medium (M), and large (L) particles. A volume fraction is associated with each population ($\phi^S$, $\phi^M$, $\phi^L$) in increasing order of size. $\phi^S$ is the volume fraction of small particles with respect to the volume of the small particles plus the continuous medium, $\phi^M$ is the volume of medium-sized particles divided by the volume of medium and small particles plus the continuous medium, and so on:

$$\phi^S = \frac{V^P_{Polym}}{V_{Water} + V^P_{Polym}} \quad (3)$$

$$\phi^M = \frac{V^M_{polym}}{V_{Water} + V^P_{polym} + V^M_{polym}} \quad (4)$$

$$\phi^L = \frac{V^L_{polym}}{V_{Water} + V^P_{polym} + V^M_{polym} + V^L_{polym}} \quad (5)$$

Further, Farris also introduced a function $H(\phi^j)$, which is the relative viscosity of phase $j$ as a function of the volume fraction of said phase. The relative viscosity of a trimodal latex will then be given by:

$$\mu_r = H(\phi^S) \times H(\phi^M) \times H(\phi^L) \quad (6)$$

Farris[20] applied this model to a system of latices with particles $> 1$ $\mu$m and used experimentally defined values of the function $H(\phi)$. Of course, one could either define other experimentally obtained functions or use the Mooney equation to define $H(\phi)$. By varying the form of these functions, Farris showed that once the ratio of diameters of two neighboring populations (e.g., S with respect to M) is greater than 10, interactions between the two populations are negligible. Under conditions where particle–particle interactions are reduced to a minimum, Farris[20] showed that one obtained a minimum viscosity for a ratio of 28% small particles and 72% large particles by volume for a bimodal latex, and a ratio of 12% small, 28% medium, and 60% large particles for a trimodal latex. This approach is interesting because it allows us to explicitly account for the contribution of different populations to the overall viscosity. Its one major weakness is that it does not take into account particle–particle interactions, and especially, electroviscous interactions.

## Experimental Approach

Experimental investigations of the effect of the PSD on latex viscosity are far more numerous than the theoretical treatments.[3,6,7,15,18,19,21–25] For instance, Chu et al.[3] carried out an experimental study on trimodal latices, which were prepared by mixing together three of four different monomodal terpolymer emulsions (styrene–butyl acrylate–methacrylic acid in the mass ratio of 66 : 33 : 1) with particle diameters of $d_p = 75$, 135, 340, and 477 nm. The different samples were concentrated by evaporation and the viscosities were measured at constant shear rates. Note that their polymers had a glass transition temperature ($T_g$) well above ambient temperature, and as

a result, the particles are not deformable, and the concentration step was relatively uncomplicated. They found that, in general, mixtures that contained particle weight fractions of approximately 80% large particles presented the lowest viscosities. In fact, they were able to create trimodal blends with a polymer content of 71.7% (mass) with a viscosity of 1077 MPa s at a shear rate of 10 $s^{-1}$ with the following proportions (mass): 80% of large (474 nm) particles, 10% medium (135 nm) particles, and 10% small (75 nm) particles.

Greenwood et al. used poly(methyl methacrylate) (PMMA)[15] and polystyrene (PS)[21] latices to study the rheology of bimodal PSDs in terms of the ratio of the diameters of large-to-small particles and the relative fraction of each population. Their experiments showed the viscosity to be at minimum when the small particles represented a volume fraction of 15–25% of the particle phase and when the ratio of large-to-small particles was 7.83.

Kemmere et al.[22] also studied the rheology of bimodal latices containing particles of 38 and 108 nm and found that the minimum viscosity was obtained at a volume fraction of 30% small particles. The ratio of large to small particle diameters in this study was less than 3, which might explain the higher optimal concentration of small particles than in the work of Chu et al.[3] and Greenwood et al.[15,21]

### Objectives

To set clear objectives for producing a high solids content latex with a minimum viscosity, it is necessary to understand the relationship between the shape of a multimodal emulsion PSD, particle concentration, and the viscosity. From the discussions presented above, we can conclude that for bi- and trimodal latices, if we can calculate a value of $\phi_{max}$ as a function of the size and quantity of the different populations in the latex, then we should be able to identify the optimum conditions (i.e., lowest viscosity for highest solids content). Therefore, in what follows, we will present an experimental study of the viscosity of bimodal and trimodal acrylic latices, as well as a numerical method that can be used to identify $\phi_{max}$ for different conditions.

## EXPERIMENTAL STUDY OF LATEX VISCOSITY

In this section, we will present an experimental examination of the viscosity of different latex blends to determine the optimal PSD in terms of minimizing the viscosity. An attempt to model the data thus obtained with different models presented above is then presented.

### Experimental

#### *Latex Preparation*

The composition of all of the latices used in this study was (by weight) 78% butyl acrylate (BA), 19.5% MMA, and 2.5% acrylic acid (AA). All materials were obtained from ACROS (France) and used as received. The latices were prepared in unseeded, semibatch reactions in a jacketed glass vessel. The recipes for the small, medium, and large particles are presented in Table II. The details of the recipes, and the reasons for choosing their compositions, are discussed by Schneider[26] and will be presented in Part II of this series.[27] The characteristics of the final latices are presented in Table III. The average particle sizes of the unmixed latices were measured by using a Malvern Lo-C quasi-elastic light scattering device. The anionic surfactant used in this study was Disponil® FES 32 IS (sodium salt of the sulfate of a polyglycol ether), and the nonionic surfactant was Disponil® A 3065 (mixture of linear ethoxylated fatty acids). Both surfactants were kindly supplied by Cognis (France) and used as received.

#### *Preparation of Latex Blends*

Different blends of the raw latices presented in Table III were prepared and concentrated as much as possible in a rotary evaporator under vacuum at ambient temperature. The evaporation step must be performed carefully and relatively slowly to prevent the formation of coagulum that can perturb the results of the rheological characterization. It was not possible to heat the mixture during evaporation because of the low $T_g$ ($\sim -30$°C) of the polymer. Samples from a given blend were progressively diluted with deionized water to be able to plot viscosity as a function of the volume fraction of polymer in the emulsion. Solids contents of the concentrated and diluted latices were measured by gravimetry. The composition in terms of proportions of particles of different sizes is presented in Table IV.

#### *Viscosity Measurements*

Viscosity measurements were performed on a Couette-type viscometer (SUCK model V10) at a

**Table II Recipes for Preparation of Small, Medium, and Large Particles**

| | Small Particles | Medium Particles | Large Particles | |
|---|---|---|---|---|
| | | Initial Charge | | |
| Temperature | 80°C | 70°C | 70°C | |
| Duration | 10 min | 18 min | 48 min | |
| $H_2O$ | 1282.4 | 872.7 | 868.8 | |
| $TA_{anionic}$ | 18.9 | 0.01 | 0.01 | |
| $TA_{nonionic}$ | 39.5 | 5 | 3.5 | |
| BA | 70.9 | 80 | 80 | |
| MMA | 17.7 | 20 | 20 | |
| Buffer | | 0.64[a] | 1.9[b] | |
| APS | 2.64 | 0.9 | 1.8 | |
| | | Semibatch Feed | | |
| Duration | 66 min | 404 min | 436 min | 308 min |
| $H_2O$ | | 302.5 | 271.8 | 129 |
| $TA_{anionic}$ | 19.9[c] | | | |
| $TA_{nonionic}$ | 41.6[c] | 29.8 | 15.8 | 7.14 |
| BA | 407 | 896 | 924 + 6.1[d] | 339.3 |
| MMA | 102 | 227 | 231 + 1.5[d] | 95.7 |
| AA | 13 | 30 | 34 + 0.2[d] | |
| APS | | 2.6 | 2 | |
| BPO | | | 1.5[d] | |

[a] $Na_2S_2O_5$.
[b] $NaHCO_3$.
[c] Added after completion as poststabilizers.
[d] Added as shot just before end.

constant temperature of 22°C. The apparent viscosity of different samples from the same batch of latex blend was measured at shear rates from 0 to 100 $s^{-1}$. Note that we have chosen to present the results of the viscosity measurements of the difference at a shear rate of 20 $s^{-1}$. Although it might be more representative to present the results at very low shear,

$$\eta_0 = \lim_{\dot{\gamma}\to 0} \eta_{app} \tag{7}$$

rather than at 20 $s^{-1}$ because the zero shear limit would give us the relationship between $\phi$ and the percolation limit. However, our samples often show a yield stress at low shear rates, which makes the extrapolation to accurate values of $\eta_{app}$ at zero shear rather inaccurate. In addition, the viscosity at 20 $s^{-1}$ is a quantity typically used in industrial situations to characterize the applicability of this type of latex.[28]

## RESULTS AND DISCUSSION

The reproducibility of the viscosity measurements was tested for different samples, and typ-

**Table III Characteristics of the Final Latexes Used in Viscosity Study**

| | Large Particles | Medium Particles | Small Particles |
|---|---|---|---|
| Solids content (vol) | 60.3% | 49.7% | 34.8% |
| Polymer Content (vol) | 59.2% | 48.7% | 29.0% |
| $N_p$ (particles/liter emulsion) | $4.68 \times 10^{15}$ | $2.25 \times 10^{16}$ | $2.38 \times 10^{18}$ |
| $d_p$ | 607 nm | 340 nm | 60 nm |

$d_p^L/d_p^S = 10$ and $d_p^L/d_p^M = 1.8$.

**Table IV Blends Used in the Viscosity Study**

| Blend Reference | Volume Fraction | | |
|---|---|---|---|
| | Small | Medium | Large |
| B1 | 0.25 | — | 0.75 |
| B2 | 0.35 | — | 0.65 |
| B3 | 0.05 | — | 0.95 |
| B4 | — | — | 1.00 |
| B5 | 0.10 | 0.10 | 0.80 |
| B6 | 0.05 | 0.15 | 0.80 |
| B7 | 0.05 | 0.05 | 0.90 |
| B8 | 0.15 | 0.05 | 0.80 |
| B9 | 0.15 | 0.10 | 0.75 |
| B10 | 0.15 | — | 0.85 |

ical results are shown in Figure 2. This figure shows that the measurements are reproducible enough that we can draw conclusions from our series of measurements.

The viscosity at a fixed shear rate of 20 $s^{-1}$ is plotted as a function of the total solids content for the series of blends defined in Table IV and shown in Figure 3. All of the curves show a slow monotonic increase of viscosity with solids content until some critical point where huge viscosity increases are observed for small increments of solid content. Intuitively, the point where the viscosity starts to increase to infinity is probably directly correlated (and close to) the $\phi_{max}$ of the particular blend.

It can be seen from Figure 3 that there is a significant difference between the rheological behavior exhibited by trimodal distributions B5, B8, B10, and that of the monomodal latex consisting only of large particles (B4). In terms of maintaining a low viscosity at high solids content, it is clearly advantageous to use a correctly formulated bi- or trimodal latex (recall that our objective is to identify the combination of particle sizes that allow us to obtain the highest solids content

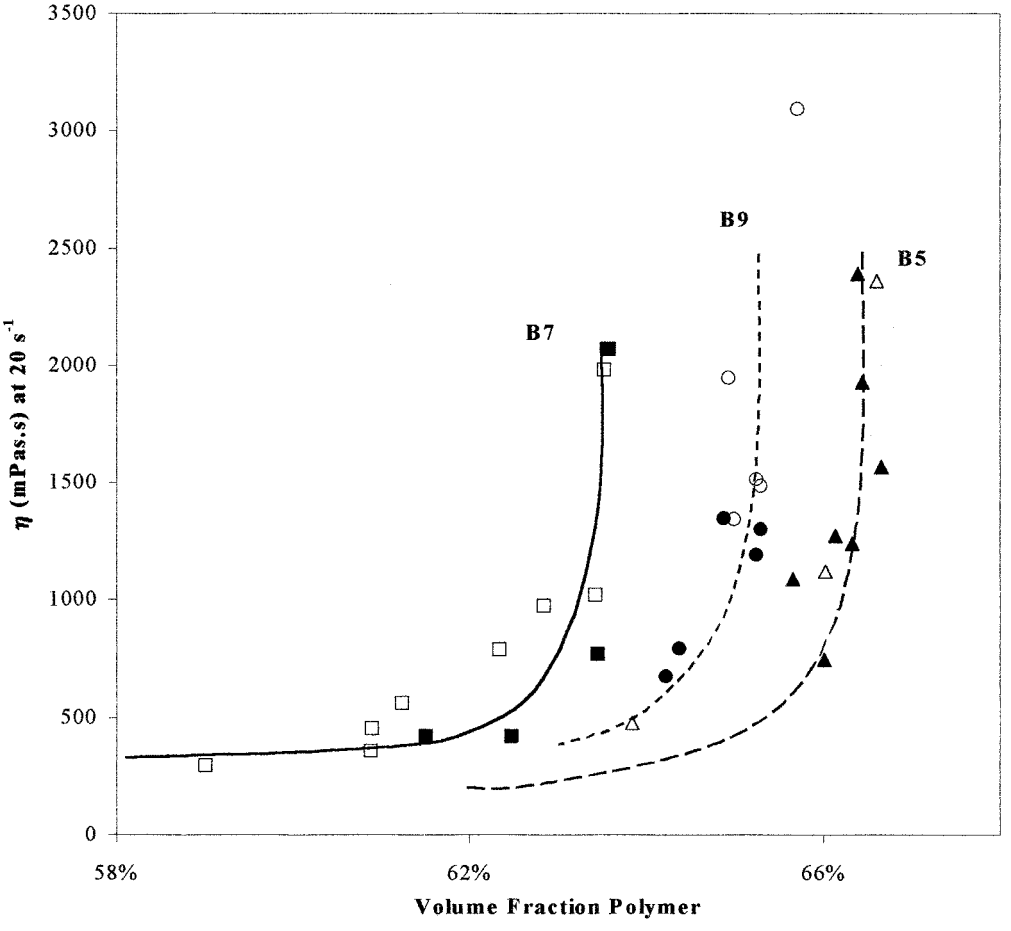


**Figure 2** Reproducibility of the viscosity measurements.

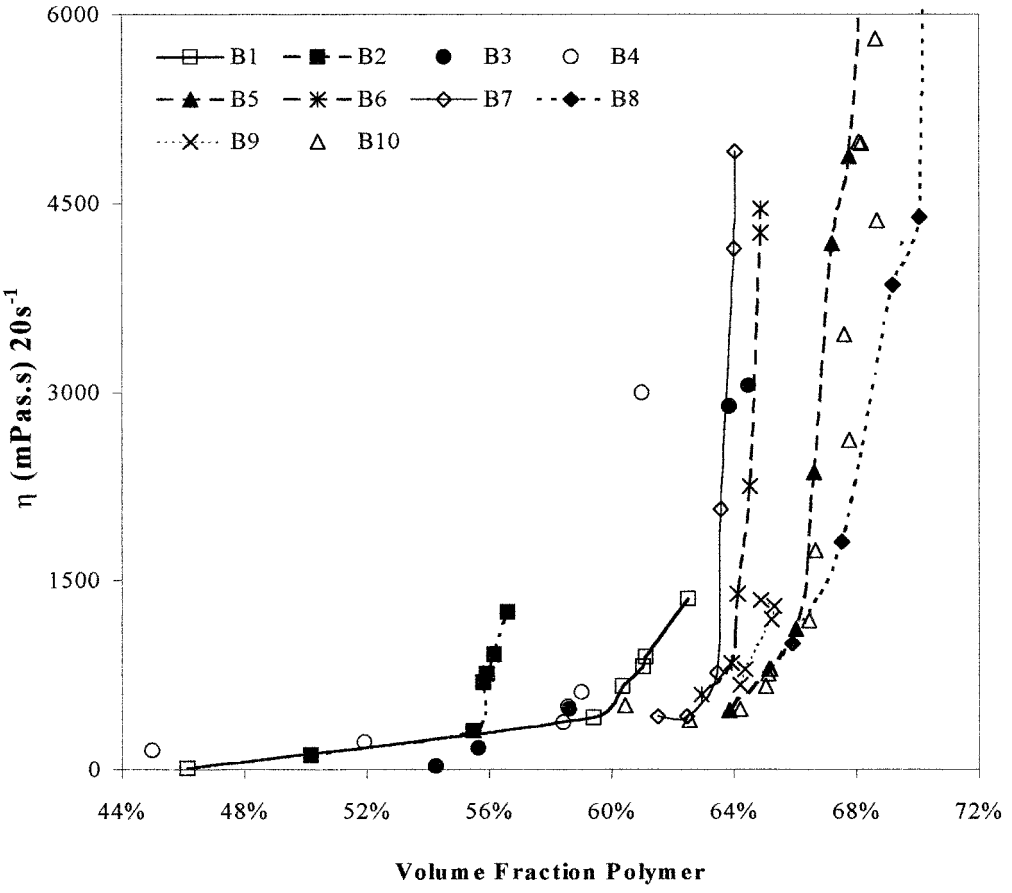


**Figure 3** Viscosity of different latex blends as a function of polymer content at 20 $s^{-1}$. For PSD information, see Table IV. Note that the curves on the graphs are simply interpolations to help differentiate between neighboring data sets. They have no physical significance.

at the lowest possible viscosity). However, it should be pointed out that producing bimodal latices does not guarantee that the viscosity will be lower for a given solids content. Comparing blend B2 to blend B4 shows that a bimodal latex with 35% small particles by volume actually has a lower viscosity than the monomodal latex, which suggests that the proportions of each population are very important. This is underlined by the fact that latex B9 has a lower viscosity for a given solids content than B1, and its maximum solids content is higher than that of B1. Both of these latices contain 75% large particles, but different quantities of the two smaller populations. In fact, replacing a part of the small particles in B1 with medium-sized particles (B9) allows us to achieve a higher solids content for the same viscosity. From Figure 3, we can see that latices with between 10 and 15% small particles, 0 and 10% medium particles, and 75 and 85% large particles can be produced at higher solids content for a given viscosity than the other blend ratios. Although the latex that allows us to attain the highest solids content at moderate viscosity is a trimodal blend (B9), the difference between the rheological behavior of this latex and that of the bimodal B10 is minimal. This is more evident from Figure 4, where we have plotted the volume fraction of each blend that corresponds to a viscosity of 1000 MPa s at 20 $s^{-1}$. The maximum volume fraction is very close to the 80% large particle–15% small particle mark and seems to drop off quickly in all directions (although with a bit of imagination, one could say that adding a small quantity of medium-sized particles might improve the solids content a very small amount).

Because the results presented here are valid only for the sizes presented in Table III, care must be taken not to overgeneralize the conclu-

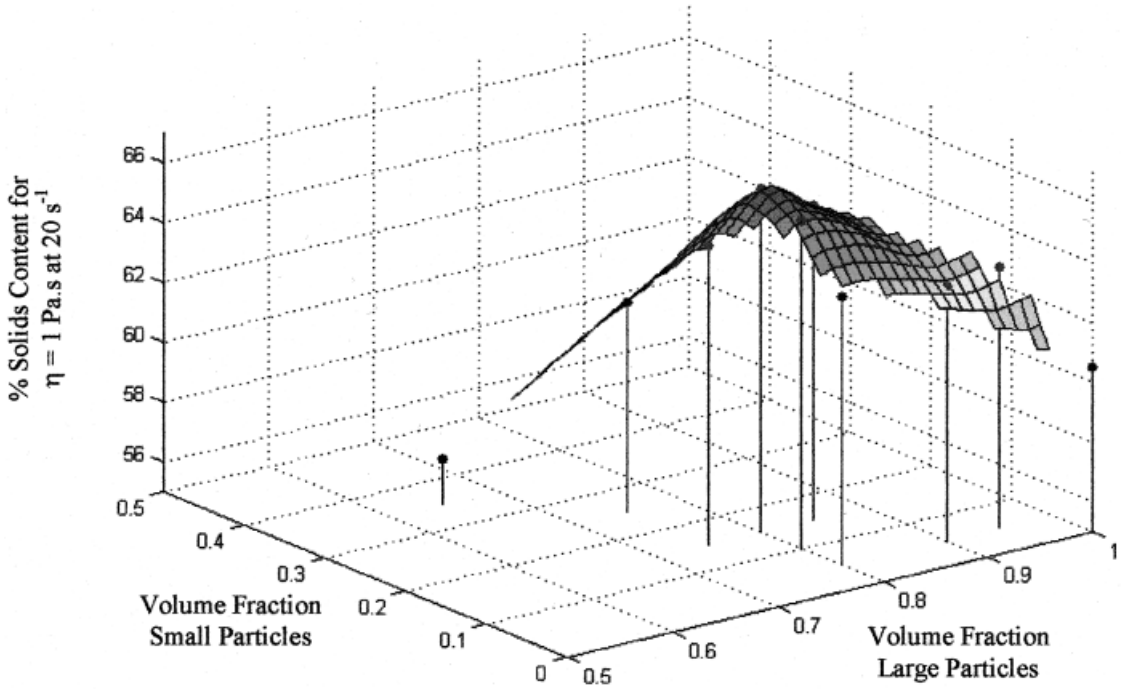


**Figure 4** Three-dimensional plot of the volume fraction corresponding to a viscosity of 1000 MPa s at 20 $s^{-1}$. Maximum value corresponds to a blend close to B5, B8, or B10. [Color figure can be viewed in the online issue, which is available at www.interscience.wiley.com.]

sions of this study to all multimodal systems (although the proportions of 80–85% large particles representing the lowest viscosity for a fixed solids content is in agreement with the literature data cited above).

## Evaluation of Viscosity Models

It would obviously be useful to have a model that allowed us to predict the viscosity of a multimodal dispersion as a function of $\phi$, and the average sizes of the different subpopulations, and, as we discussed above, several are presented in the literature. In this section of the article, we will try to model the data presented above with three of the equations presented in Table I.

### *The Mooney Model*

This model was developed for monomodal dispersions of hard, nondeformable spheres and does not take the PSD directly into account. It does, however, include the term $\phi_{max}$, which, if we can identify a value for the different latices, might allow us to use the models in a predictive manner. As we can see in Figure 5, the Mooney model can be made to fit the data from different runs by adjusting the value of the parameter $\phi_{max}$. Two problems arise, however. (1) The fitted values of $\phi_{max}$ are very different from the values of $\phi_{max}$ (or rather the limiting solids content), shown in Figure 3 for the different blends. The fitted values range from 0.767 for the monomodal latex to 0.88 for one of the trimodal latices, whereas the limiting solids content in Figure 3 range from approximately 0.63 (not clear for B4) to 0.7. (2) We have no means of predicting these values *a priori*, and the value of 0.767 is much higher than what one might logically expect for a monomodal system. Of course, blend B4 is not perfectly monodisperse, and as we will see in the next section, broadening the PSD can help to lower the viscosity (or equivalently, increase $\phi_{max}$). However, it seems highly unlikely that a packing factor of 0.767 has any physical sense for a monomodal system, especially under dynamic conditions. Of course, the Mooney equation was not developed for this type of multimodal system with potential particle–particle interaction (via the presence of stabilizers), so it is understandable that the model does not function as a predictive model.

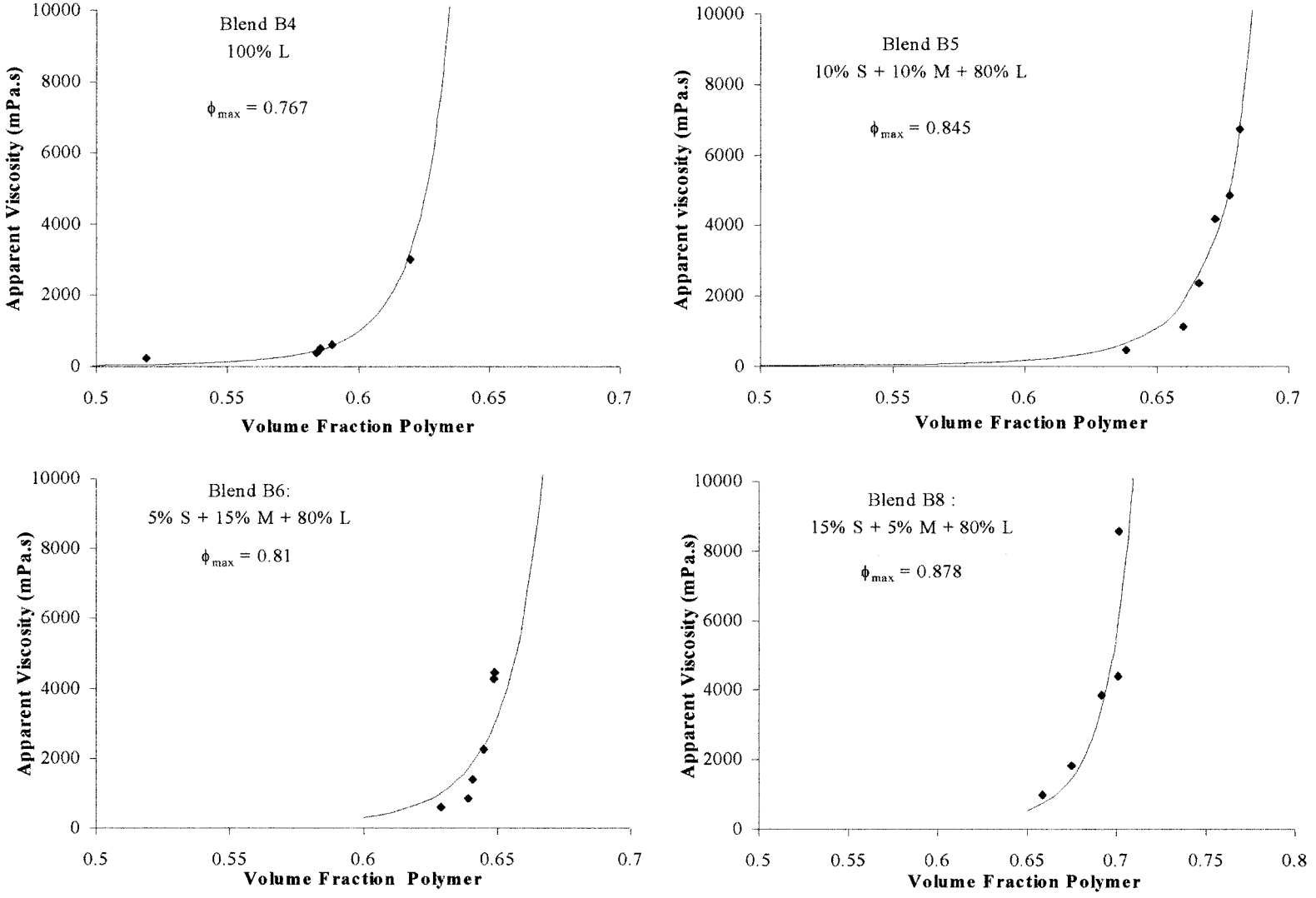


**Figure 5** Apparent viscosity modeled using the Mooney equation. Note that to fit the data, extremely high (and physically unrealistic) values of $\phi_{max}$ are needed. Viscosities are shown at a shear rate of 20 $s^{-1}$.

**Table V Optimized Parameters for the Krieger–Dougherty Model**

| Blend | $\phi_{max}$ | $[\eta]$ |
|---|---|---|
| 1 | 0.713 | 4.850 |
| 2 | 0.586 | 3.625 |
| 3 | 0.687 | 3.917 |
| 4 | 0.658 | 4.256 |
| 5 | 0.704 | 3.873 |
| 6 | 0.658 | 2.983 |
| 7 | 0.645 | 2.718 |
| 8 | 0.731 | 3.780 |
| 9 | 0.704 | 3.889 |
| 10 | 0.727 | 4.188 |

### *The Krieger–Dougherty Model*

If we consider the Krieger–Dougherty model, we can see immediately that such high values of $\phi_{max}$ would lead to an underprediction of the viscosity because of the form of the equation. Second, this equation also includes the intrinsic viscosity of the latex as a model parameter. The intrinsic viscosity $[\eta]$ is an important parameter in this and some of the other models presented in Table I and is defined as:

$$[\eta] = \lim_{\phi \to 0} \left[ \frac{1}{\phi} (\eta_r - 1) \right] \tag{8}$$

In conditions where the simplifying hypotheses of the Einstein model apply, $[\eta] = 2.5$. We attempted to directly measure the viscosity of a latex diluted to 0.2 vol % fraction on a low-shear cone and plate viscometer (access was kindly provided by the Laboratoire de Physicochimie Macromoléculaire at the ESPCI in Paris, France). Unfortunately, the error in the measurements ($\pm 5\%$) was the same order of magnitude as the difference between the viscosity of the diluted latex and water. A capillary viscometer would perhaps have been better adapted to this measurement, but we did not have access to such a device during the course of this study. For that reason, we will ultimately be led to treat $[\eta]$ as an adjustable parameter (because using an intrinsic viscosity of 2.5 in the Dougherty equations does not allow us to fit the data). The results of a nonlinear least-squares (Matlab® Optimisation Toolbox, *leastsq* function) fit of the viscosity data (at 20 $s^{-1}$) of the Krieger–Dougherty model are presented in Table V. The values of $\phi_{max}$ determined for this model are obviously much more reasonable that the values presented for the Mooney equation, and, if we compare with Figure 3, are directly correlated with the point where the curve $\eta(\phi)$ tends toward infinity. It can also be noted that the intrinsic viscosities are between 2.72 and 4.85, slightly higher than the value of 2.5 in the Einstein equation. However, they are also quite reasonable, as the value of 2.5 is for nondeformable, noninteracting spheres, and in the case of our latex, neither of these hypotheses (especially the second) is true. In addition, given that the recipe contains acrylic acid, monomer, and of course, surfactants, it is highly probable that the continuous phase contains water-soluble polymers which will also influence the true value of $[\eta]$. It should also be pointed out that these models are in fact zero-shear models, whereas our measurements were done at a nonzero shear rate.

### *The Farris Model*

The Farris model is (in principle) the only one presented in Table I that allows us to calculate directly the contribution of each population in the blend to the overall (apparent) viscosity of the dispersion. However, because the polymodal latices with which we are concerned contain relatively high volume fractions of large particles, the prediction of the Farris model is dominated by the value of $H(\phi^L)$ for the large population. In fact, a series of calculations (not shown here for reasons of brevity) reveals that, with the exception latex B2 where the small particles are fairly numerous, the results for the model predictions are entirely independent of the volume fractions of small and medium particles and depend only on the model chosen for the large population. It was found that if we use the Mooney equation for the $H(\phi)$ in eq. 6, the values of $\phi_{max}$ for the large populations are very close to those in Table V for the Krieger–Dougherty model and more reasonable than the values presented in Figure 5. Nevertheless, we remain confronted with the problem of how to estimate $\phi_{max}$ if we wish to use one of the existing viscosity models. We will propose a method of getting around this problem in the following section.

## SIMULATION OF THE RANDOM PACKING OF SPHERES

Two important points should be clear from the preceding sections.

1. The viscosity of a multimodal latex is highly sensitive to the PSD, and we do not know the relationship between the PSD (number of populations, average $d_p$ of each population) and the viscosity.
2. Similarly, predictive models of the viscosity require *a priori* knowledge of the parameter $\phi_{max}$, which is very difficult to calculate.

In this section, we will propose a method based on the calculation of a the relationship between the PSD and the maximum volume fraction occupied by spheres that randomly fall into a container. The idea is to develop an approach that will allow us to directly simulate the relationship between the PSD and the parameter $\phi_{max}$, or at least a value $\phi_{lim}$ that approaches $\phi_{max}$ and that represents the highest volume fraction of solids attainable by letting particles fall into a large boxlike container. In theory, the PSD that gives us the highest packing factor $\phi_{max}$ should also give us the lowest viscosity possible at a given volume fraction, and if we can approximate $\phi_{max}$ by $\phi_{lim}$, we should be able to identify the optimal PSD in terms of viscosity. We will define these two terms as follows. $\phi_{max}$ is the maximum volume fraction obtainable with optimal packing of particles (e.g., 0.74 for uniform spheres and faced-centered cubic packing, or 0.64 with random packing). $\phi_{lim}$ is the maximum volume fraction obtainable with the random packing (between 0.52 and 0.74) given the constraints imposed by the simulation routine described below. Note that both $\phi_{lim}$ and $\phi_{max}$ can take on different values in the event that particles are randomly packed. As we will see below, there are some subtle differences between $\phi_{lim}$ and $\phi_{max}$, not least because calculating $\phi_{max}$ implies that when particles are being randomly packed, they can be displaced in any direction. In the simulations presented below, the particles are dropped into a box and will continue to fall until they are supported either by the bottom of the container (for the first layers) or by at least three other particles. If the particles fall and touch one or two other particles, they are displaced horizontally a certain distance that allows them to continue their trajectory until they come to rest. This type of calculation can create situations (for multimodal latices) where there are void spaces in the packing that would be large enough to accommodate certain particles, and thus, the maximum packing factor $\phi_{lim}$ will be less than (or at best equal to) $\phi_{max}$. Nevertheless, as we will show below, the results of this type of simulation are coherent with experimental results (both those presented here and those reported in the literature).

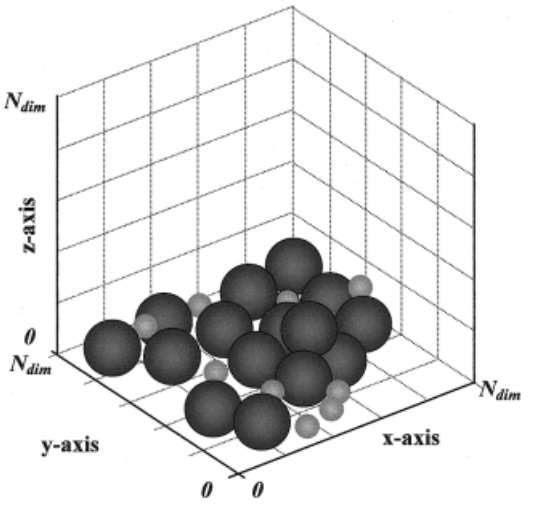


**Figure 6** Schema of format for simulation of random packing and estimation of $\phi_{lim}$ for the case of a bimodal latex.

## Calculation Algorithms

The algorithms presented in this section are designed to calculate the volume fraction of solids obtained by filling a boxlike container with spheres that are randomly dropped into it. To render the simulations tractable, we will impose certain simplifications:

- All particles are rigid, noninteracting spheres;
- We will not consider more than three populations;
- Each population is considered to be monodisperse.

All simulations were written and run in C++.

The space to be filled is shown schematically in Figure 6. It is a cube of dimension $N_{dim}$, with each cell being assigned a number between 0 and ($N_{dim}$ − 1). In the case of a multimodal latex, a cell is assigned a dimension equal to the radius of the smallest particle. In fact, $\phi_{lim}$ is calculated in this cube, but the container is actually filled to a height of $2N_{dim}$ to avoid problems linked to the formation of a pile in the middle of the cube, with void spaces near the wall. The simulation begins

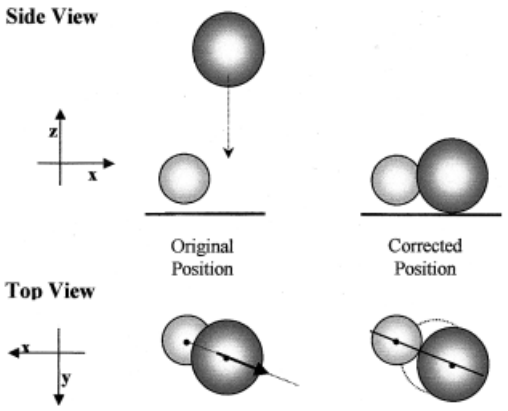


**Figure 7** Displacement of a falling sphere to account for the presence of a single potential contact. Note that original particle (light shading) is at a random height of less than one particle radius above the surface of the box, as described above.

by dropping a particle into the cube. Both the coordinates of the starting point of the drop and the size of the particles (in the case of multimodal latices) are chosen randomly. In the case of a multimodal latex, the PSD is predefined in terms of the size and relative proportions of two or three populations. As an example, in the case of a bimodal latex, define $f_1$ to be the number fraction of small particles. The size of the particle to be dropped is then chosen by generating a random number between 0 and 1. If the number is between 0 and $f_1$, the particle to be dropped is a small one; otherwise, it is a large one. Similarly, the $x$ and $y$ coordinates of the particle are also chosen with a random number generator. However, to avoid biasing the results by the formation of a perfectly uniform initial layer, particles are initially assigned a final $z$-coordinate between 0 and 1, also through the generation of a random number. This coordinate is used only if the particles in question do not come to rest on three other particles, but rather fall to the bottom of the box.

Once a particle has been chosen and is dropped, it will continue to fall toward the original $x$-$y$ coordinates until it encounters either another object or the $x$-$y$ plane. If it encounters another sphere, it is displaced horizontally until it comes to rest on the $x$-$y$ plane or until it comes into contact with at least three other points of contact. Once the particle comes to rest, its coordinates are fixed and it can no longer be moved; however, it can be displaced while it is falling. To simplify the calculations, we have imposed the following limitations on the arrangement of the particles in the cube:

1. The falling particle enters into contact with one particle. As shown in Figure 7, in the case where a falling particle (PF) enters into contact with one particle (P1), it is displaced along the axis formed by the straight line drawn through the centers of both particles until its center is at a distance $(r_1 + r_F)$ from the fixed particle, where $r_1$ and $r_F$ are the radii of P1 and PF, respectively. It then either remains there if it is in the first layer [the situation in schema Fig. 7(a)], or continues to fall until it either encounters another particle or its $z$-coordinate is equal to the $z$-coordinate that it was randomly assigned to when released into the box. This case applies if no other particle is detected inside the sphere with its origin at the center of P1 and a radius $(r_1 + r_F)$; otherwise, we go to scenario 2 below.

2. The falling particle can enter into contact with two particles. In Figure 8, the schema is adapted to a falling particle (PF) that can encounter two fixed particles. In this case, we have detected only one existing particle that occupies part of the space defined by the tangent sphere around P1. The center of the falling particle is then displaced on the tangent sphere in such a way that its center remains on along the axis defined by the $x$ and $y$ coordinates of the centers of P1 and PF at the moment of contact. The particle descends until its center arrives on the surface of the tangent sphere with its origin at the center of P2 and with a radius $(r_2 + r_F)$. After this point, the center of PF is displaced along the curve defined by the intersection of the two tangent spheres until the $z$-coordinate of its center is less than that of the $z$-coordinate of either P1 or P2

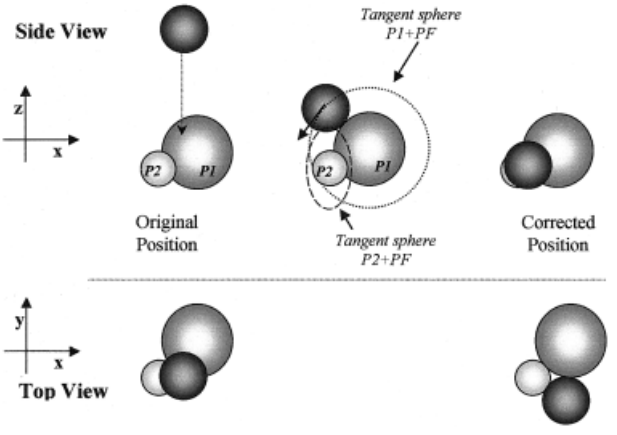


**Figure 8** Displacement of a falling sphere (PF in black) that contacts two fixed spheres (first P1, then P2).

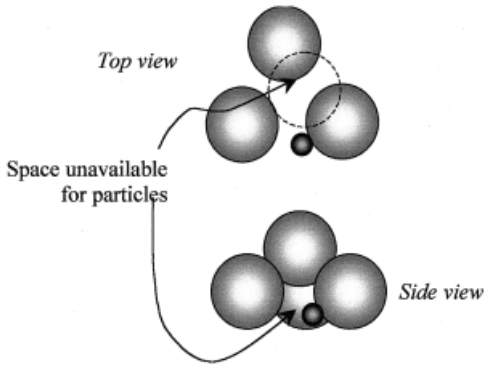


**Figure 9** Underinitialization of space in the random packing of spheres due to immobility of particles at rest.

(whichever occurs first). We then revert to scenario 1 above.

3. The falling particle can enter into contact with three particles. As above, PF follows the tangent sphere defined in common with P1, then, continues along the intersection between the tangent spheres P1 + PF and P2 + PF, as above, until the particle intersects the sphere defined by PF and P3 (the third particle with which PF comes into contact). At this point, two things can happen. If the center of gravity of PF lies inside the triangle defined by the contact points (in the $x$-$y$ plane), the particle comes to rest in its final position. Otherwise, if the center of gravity of the particle lies outside this triangle, PF will fall along the curve defined by the intersection of spheres PF + P2 and PF + P3.

Of course, we are aware that this means of calculation will not provide an exact value of $\phi_{max}$ because the particles cannot rearrange themselves once they have come to rest. As shown in Figure 9, the fact that the particles cannot move means that a certain amount of space (especially in the first few layers of the cube) will be underutilized. For instance, in this figure, if we imagine that the four large particles have fallen and occupied the space shown, the small particle must fall outside the space defined by the larger ones even though in theory it could be inserted in the interstices indicated by the arrows. Nevertheless, if the cube to be filled is big enough, the PSD that gives us the highest value of $\phi_{lim}$ will in all probability be the one that corresponds to the highest value of $\phi_{max}$, and thus, the lowest value of $\eta$ at a given solids content.

In addition, one must also consider problems related to the overlapping of particles with the external boundaries of the cube. To get around this sort of problem without writing stringent boundary conditions, we assumed the cube was repeated periodically in the $x$-$y$ plane. For instance, as shown in Figure 10, it is necessary to sweep the shaded space in the left-hand image to detect the presence of secondary particles with which a falling particle would come into contact.

## Simulation Results

The results of the simulations reported in this paragraph are the average of at least 20 simulations per point. The reason for this is, as mentioned above, there can be no single value for a random packing factor, so it is possible that it will vary from simulation to simulation. In addition, we also wished to avoid anomalous predictions due to an overabundance of situations such as those presented in Figure 9.

Initial simulations were run to determine the minimum value of $N_{dim}$ necessary to assure that the simulations were independent of the size of the cube and of $d_p$. It was found that in order for the final result to be independent of particle size,

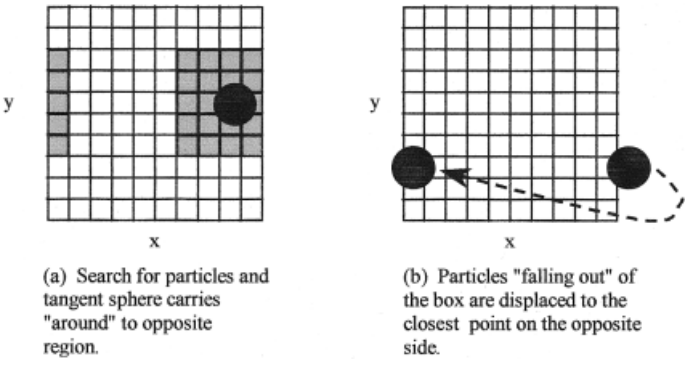


**Figure 10** Assumed periodicity of space used to avoid edge effects.

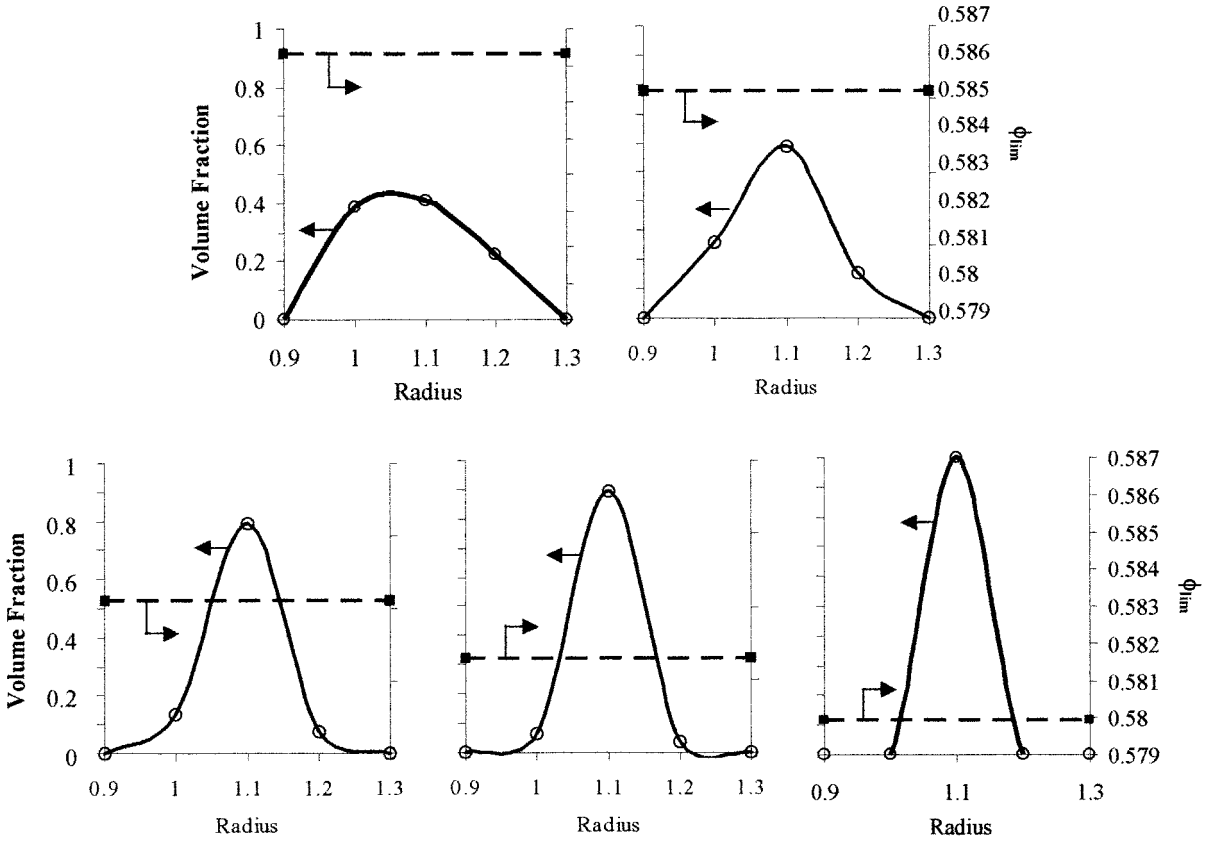


**Figure 11** Effect of the width of the PSD on the value of $\phi_{lim}$ for a monomodal latex.

$N_{dim}$ must be at least 20 times larger than the largest particle in the system. For example, if we consider a bimodal latex with a ratio of 10 between the diameter of the large and small particles, $N_{dim}$ must be at least 200 in order for this condition to be respected.

### *Influence of the Width of the PSD of a Monomodal Latex*

Before considering truly bi- and trimodal latices, we examined the influence of the width of the PSD of a monomodal latex on $\phi_{max}$. Because we have imposed the condition that individual populations must be monodisperse, this is done by performing the simulation for a trimodal latex with very similar radii (1, 1.1, 1.2) in different proportions. As we can see from Figure 11, the values of $\phi_{lim}$ are lower than the value of 0.64 that one might expect to find in this type of simulation. However, as we mentioned above, this can be attributed to the immobility of the particles at rest, and therefore, the underutilization of the space in the container. Nevertheless, these simulations clearly show that as the PSD broadens, the value of $\phi_{lim}$ increases. This result is coherent with what we would expect to find.

### *Bi- and Trimodal Distributions*

The results of a simulation for a purely bimodal distribution with a particle size ratio, $R_L/R_S = 2$ (large particle radius divided by small particle radius), are shown in Figure 12. The results of the simulation are in good agreement with the experimental data reported in the literature (see above), with a maximum volume fraction of solids being approached for a volume fraction of small particles between 0.25 and 0.3 (maximum of a second-order fit at $\phi_S = 0.3$ and for a third-order fit $\phi_S = 0.26$).

Note that each point on Figure 12 is an average value of at least 20 simulations. It is clear that this is not enough and that a more representative graph would be obtained with a much larger number of simulations per point. However, a significantly higher number of calculations was not possible in this instance because this graph was established

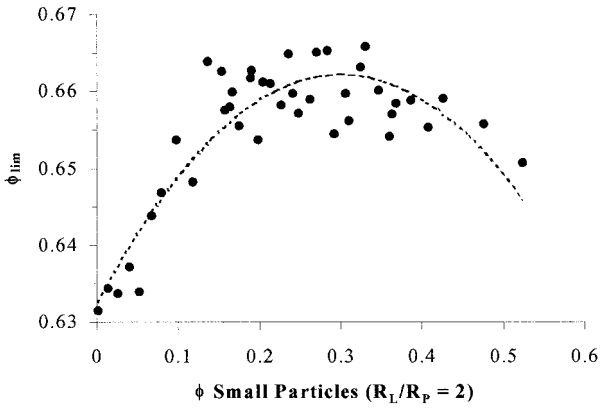


**Figure 12** $\phi_{lim}$ as a function of the volume fraction of small particles for a bimodal latex. Ratio of the radius of large-to-small particles fixed at 2. The curve is simply a second-order polynomial fit to the data to visualize the results of the simulation and has no physical basis.

with an early, nonoptimized version of the code and it was necessary to reduce the time necessary for computation. The ratio $R_L/R_S = 2$ was also chosen to reduce the time needed for the computations. As mentioned above, the size of the cube is governed by the size of the largest particles: for the case $R_L/R_S = 10$, $N_{dim} = 200$, and we need to fill a cube with dimensions of $200 \times 200 \times 400$ (height $= 2N_{dim}$). For $R_L/R_S = 2$, the cube need only be $40 \times 40 \times 80$, which means 125 times fewer calculations. The optimization of the code consisted of improving the search algorithm for the number of contact points and reducing the computation time dramatically. The improved algorithm was used for the simulations reported below.

A second series of simulations was run for a series of trimodal latices with the following size ratios: $R_L/R_S = 10, R_L/R_M = 7.7, R_M/R_S = 1.3$. The results are shown in Figure 13. Direct validation of the simulation with the experimental results in Figure 4 is not possible given that the size ratios of the particles is somewhat different. Generally speaking, the results are nevertheless coherent. If we compare Figure 4 to Figure 13, we can see that the results of the experiments and simulations show the same trends: a maximum solids fraction is reached for 75–80% large particles per unit volume. It is interesting to note that the simulations predict that, for the size ratios considered here, a bimodal mixture of large and medium particles (75% large to 25% medium) allows us to attain the highest value of $\phi_{lim}$, and although the

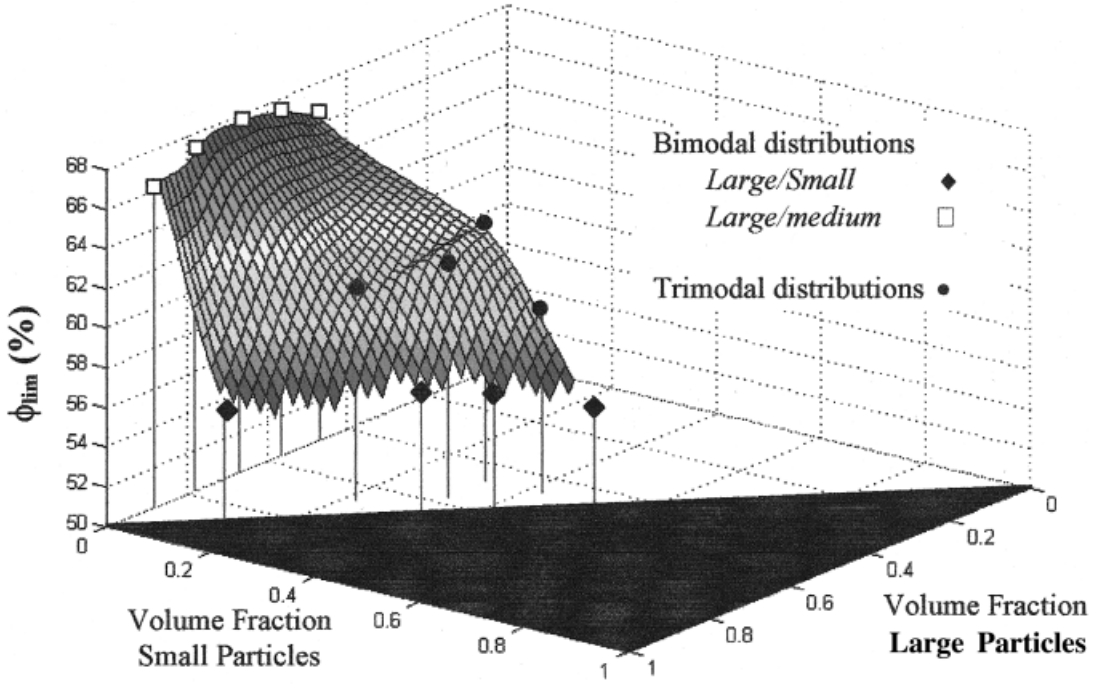


**Figure 13** $\phi_{lim}$ calculated for trimodal latices with size ratios $R_L/R_S = 10$, $R_L/R_M = 7.7$, $R_M/R_S = 1.3$. [Color figure can be viewed in the online issue, which is available at www.interscience.wiley.com.]

trimodal mixtures are better than the bimodal mixtures of small and large particles, they are not as good as a bimodal mixture of large and medium particles. Note that the ratio $R_I/R_M = 7.7$ is very close to the optimum ratio of 7.83 found by Greenwood et al.[15,21] in their studies on viscosity.

This last result suggests that the value of $\phi_{lim}$ calculated with the simulations proposed here are directly correlated to the viscosity of a bi- or trimodal latex: the PSD that corresponds to the highest values of $\phi_{lim}$ seems to correspond to the lowest viscosity. This conclusion should, of course, be applied with caution because we have only simulated a limited number of cases and have only a minimal experimental validation.

## CONCLUSIONS

The results of this experimental and modeling study allow us to draw a number of conclusions concerning the relationship between the rheology (viscosity) of multimodal latices and their PSD.

A comparison of the viscosity of blends of latices with different sizes allowed us to identify an approximate PSD in terms of the proportions of each population that allowed us to achieve relatively low viscosities ($\eta_{app}$ at 20 $s^{-1} < 1000$ MPa s). For ratios

$$\frac{d_p^L}{d_p^S} = 10 \quad \text{and} \quad \frac{d_p^L}{d_p^M} = 1.8$$

it was found that between 10 and 15% (v/v) of small particles, 0 to 10% of medium-sized particles, and between 75 and 80% of large particles provided the lowest viscosities for a total solids content of over 65%. These proportions are valid only for the size range studied here. Simulations of the relationship between the PSD and a limiting solids content suggest that this size range could be altered to achieve even higher concentrations of polymer while retaining the same rheological characteristics.

In the case of bimodal blends, the results presented here are in agreement with those in the literature, but little information is available elsewhere to confirm the results obtained for the trimodal latices.

Models of latex viscosity available in the literature can be made to fit the experimental data, but if these models are to be predictive, the value of $\phi_{max}$, the maximum solids content attainable for a given PSD, must be known *a priori*. The experimental and simulation studies showed that this parameter is highly sensitive to the PSD and is very difficult to identify without extensive experimental investigations.

The values of $\phi_{lim}$ obtained in the simulations are lower than values of $\phi_{max}$ for randomly packed spheres. This is not unexpected as no attempt was made to reproduce the same packing conditions as would be encountered in a real fluid (e.g., particles will not move horizontally underneath other particles). Nevertheless, the simulations appear to allow us to identify the proportions of different particle populations in a multimodal latex that correspond to the highest packing fraction possible. In situations where experimental results on similar systems are available, the values of $\phi_{lim}$ correspond closely to the values of $\phi_{max}$. For example, the results from Figure 13 suggest that the simulations are valid and that the PSD that corresponds to the highest value of $\phi_{lim}$ also corresponds to the lowest viscosity attainable for a given solids content.

The authors thank Atofina (CERDATO) for the financial support of this work, and in particular, Dr. Bétrémieux for helpful discussions. In addition, we are grateful to Jean Delavilléon of the CERDATO for help in performing the packing simulations.

## REFERENCES

1. Chu, F.; Graillat, C.; Guyot, A. J Appl Polym Sci 1998, 70, 2667.
2. Chu, F.; Guillot, J.; Guyot, A. Polym Adv Technol 1998, 9, 844.
3. Chu, F.; Guillot, J.; Guyot, A. Colloid Polym Sci 1998, 276, 305.
4. Pawar, V. B. Chem Eng 1997, January, 123.
5. Goodwin, J. W. in An Introduction to Polymer Colloids; Candau, F.; Ottewill, R. H., Eds.; Kluwer Academic Publishers: Dordrecht, Netherlands, 1990; pp 209–223.
6. Schaller, E. J. in Emulsion Polymerization and Emulsion Polymers; Lovell, P. A.; El-Aasser, M. S., Eds.; John Wiley and Sons: New York, 1997; Chapter 13.
7. Jinescu, V. V. Int Chem Eng 1974, 14, 397.
8. Tadros, T. F. Solid/Liquid Dispersions; Academic Press: London, 1987.
9. Vand, V. Nature 1945, 155, 364.
10. Mooney, M. J Colloid Interface Sci 1951, 6, 162.
11. Krieger, I. M.; Dougherty, T. J. Trans Soc Rheol 1959, 3, 137.

12. Quemada, D. Rheol Acta 1978, 17, 632, 653.
13. Ottewill, R. H. in Emulsion Polymerization and Emulsion Polymers; Lovell, P. A.; El-Aasser, M. S., Eds.; John Wiley and Sons: New York, 1997; Chapter 3.
14. Bicerano, J.; Douglas, J. F.; Brune, D. A. J Macromol Sci, Rev Macromol Chem Phys 1999, C39, 561.
15. Greenwood, R.; Luckham, P. F.; Gregory, T. J Colloid Interface Sci 1997, 191, 11.
16. Seife, C. Science 2000, 287, 1912.
17. Cipra, B. Science 1998, 281, 1267.
18. Sudduth, R. D. J Appl Polym Sci 1993, 48, 37.
19. Sudduth, R. D. J Appl Polym Sci 1993, 50, 123.
20. Farris, R. J. Trans Soc Rheol 1968, 12, 281.
21. Greenwood, R.; Luckham, P. F.; Gregory, T. Colloids Surf A 1998, 144, 139.
22. Kemmere, M. F.; Meuldijk, J.; Drinkenburgh, A. A. H.; German, A. L. Polym React Eng 1998, 6, 243.
23. Zecha, Z. Habilitationsschrift; Technische Universität Dresden, 1992.
24. Peters, A.; Overbeek, G. C.; Buckmann, A. J. P.; Padget, J. C.; Annable, T. PPC 1996, 38.
25. Sadler, L. Y.; Sim, K. Chem Eng Prog 1991, 69.
26. Schneider, M. Etude de Procédés de Synthèse de Latex Multipopulés à Haut Extrait Sec; Ph.D. thesis, Université Claude Bernard Lyon-I, 2000.
27. Schneider, M.; Graillat, C.; Guyot, A.; McKenna, T. F. J Appl Polym Sci to appear.
28. Betrémieux, I. (Atofina), personal communication, February 2000.